

Supporting Information

Highly Flexible Ni-Co MOF Nanosheets Coated Au/PDMS Film based Wearable Electrochemical Sensor for Continuous Human Sweat Glucose Monitoring

Yun Shu,^{a,*} Zhenjiao Shang,^a Tong Su,^a Shenghao Zhang,^a Qin Lu,^a Qin Xu,^a Xiaoya Hu^{a,*}

^a*School of Chemistry and Chemical Engineering, Yangzhou University, Yangzhou 225002, P.R.China*

**Corresponding author. Email: shuyun@yzu.edu.cn, xyhu@yzu.edu.cn*

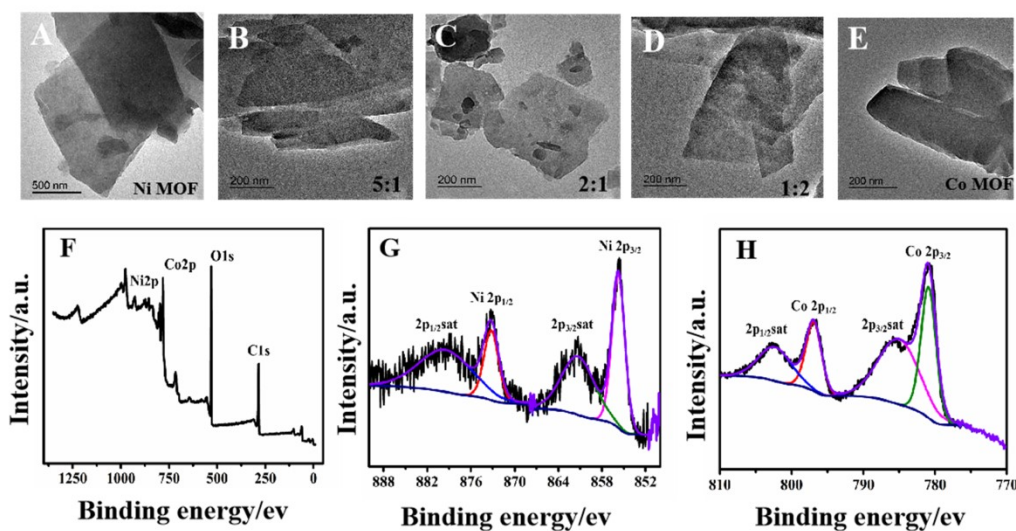


Figure S1. (A-E) TEM images of MOF products synthesized under different ratios of nickel and cobalt. (F) XPS spectra of the Ni-Co MOF nanocomposite. Corresponding spectra of Ni (G) and Co (H).

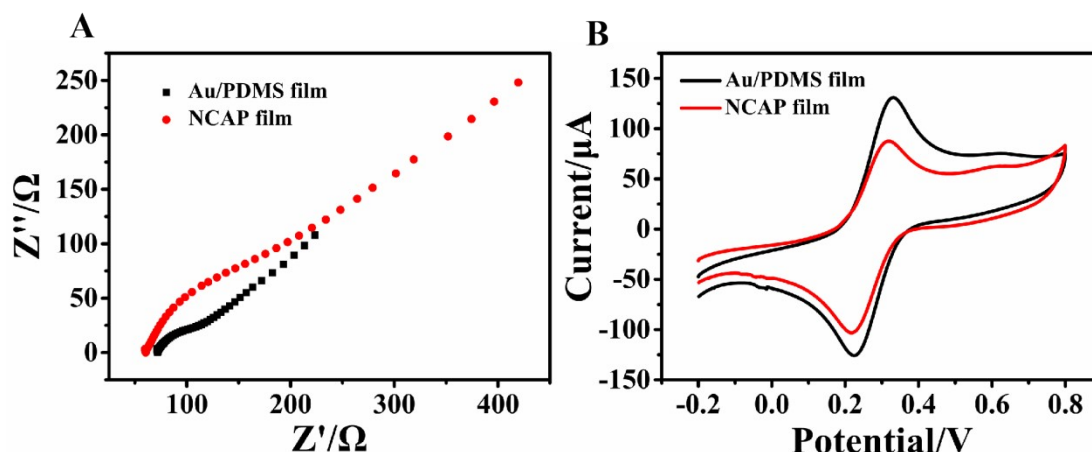


Figure S2. (A) The electrochemical impedance spectroscopy of Au/PDMS and NCAP film electrode conducted at open circuit voltage in the frequency range of 100 kHz to 0.01 Hz in potassium ferricyanide solution containing 1 M KCl and 2.5 mM $\text{K}_3[\text{Fe}(\text{CN})_6]$ and $\text{K}_4[\text{Fe}(\text{CN})_6]$. (B) CV study of Au/PDMS and NCAP film electrode in potassium ferricyanide solution containing 1 M KCl and 2.5 mM $\text{K}_3[\text{Fe}(\text{CN})_6]$ and $\text{K}_4[\text{Fe}(\text{CN})_6]$. Scan rate: 100 mV/s.

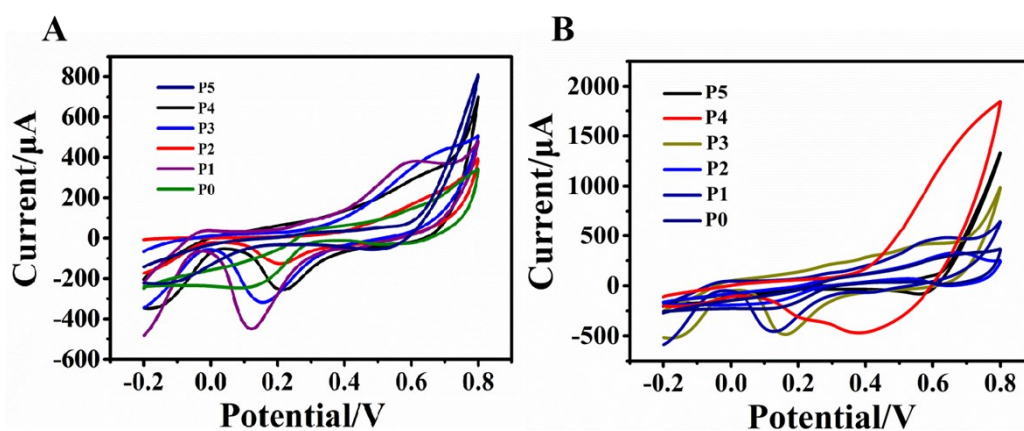


Figure S3. CV curves of flexible of Au/PDMS film electrode modified with MOF products synthesized under different ratios of nickel and cobalt in N_2 saturated 0.1 M NaOH without glucose (A) and in presence of 0.5 mM glucose (B).

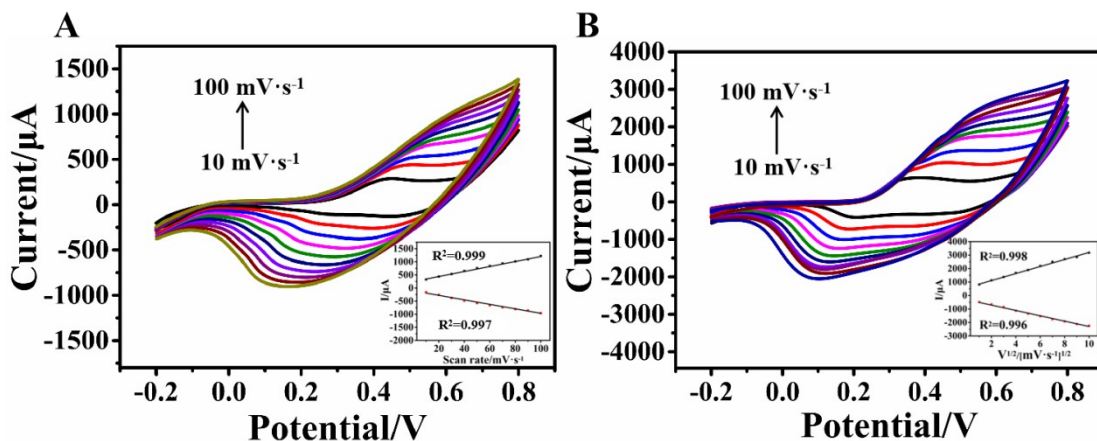


Figure S4. (A) CV curves of NCAP film electrode in 0.1 M NaOH at different scan rates (10–100 $\text{mV}\cdot\text{s}^{-1}$). Inset: the calibration curves of oxidation and reduction peak currents with the scan rate. (B) CV curves of NCAP film electrode in presence of 1 mM glucose at different scan rates (10–100 $\text{mV}\cdot\text{s}^{-1}$). Inset shows the corresponding calibration plots of oxidation and reduction peak currents with the square root of scan rates.

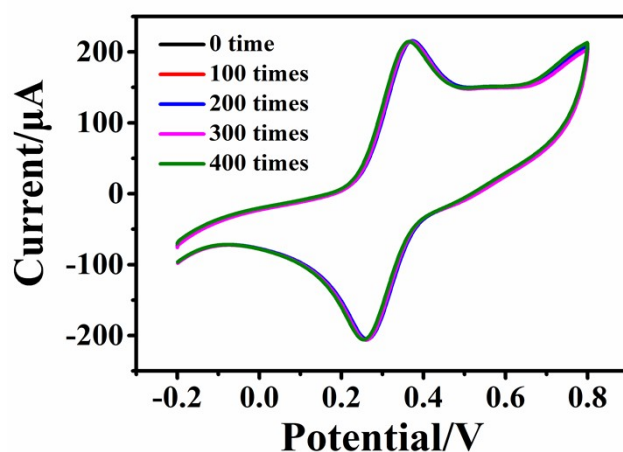


Figure S5. CV curves of the flexible sensor after cyclic stretching from 0 time to 400 times in potassium ferricyanide solution.

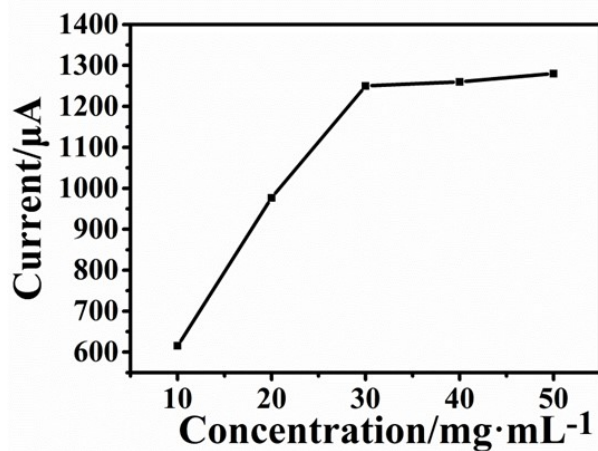


Figure S6. Influence of Ni-Co MOF with different concentrations on the response of NCAP film electrode in 0.1 M NaOH solution with 0.5 mM glucose.

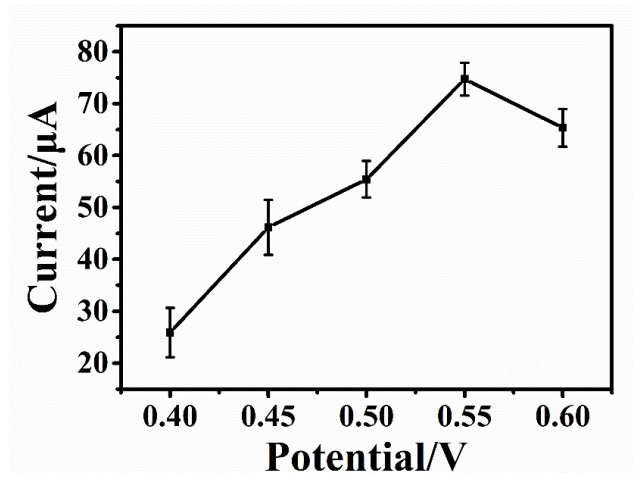


Figure S7. Amperometric study of NCAP film electrode in the presence of glucose at different potentials.

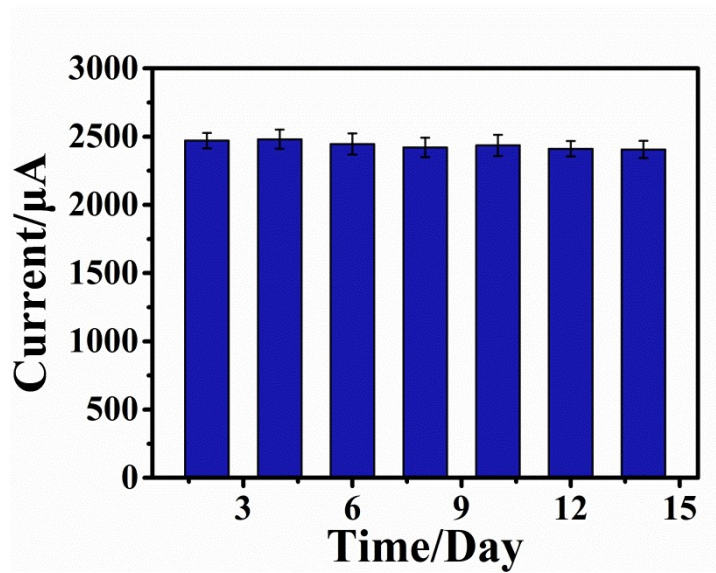


Figure S8. Variation of the current response to 1 mM glucose for NCAP film electrode versus storage time.

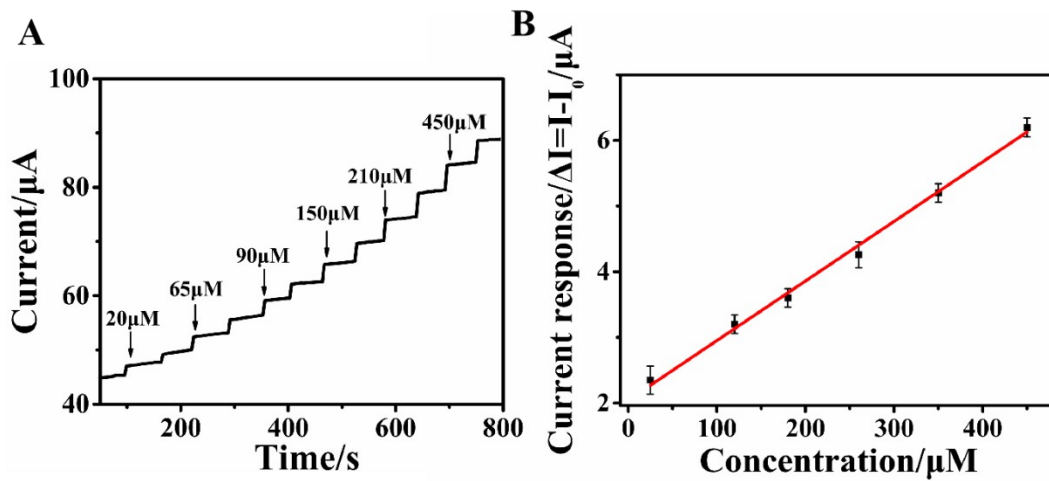


Figure S9. (A) Amperometric curve of NCAP film electrode to a serial of glucose concentration in PBS. (B) The corresponding calibration plots of current versus glucose concentration.

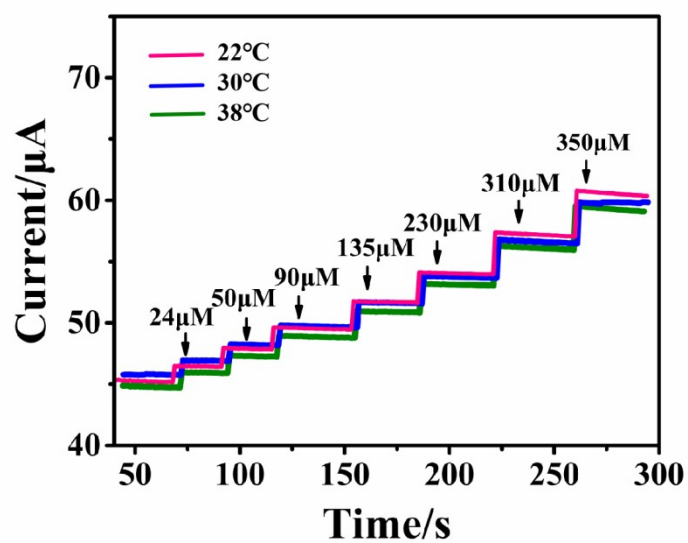


Figure S10. Amperometric curves of the NCAP film electrode at various glucose concentrations at temperatures of 22, 30, and 38 °C.

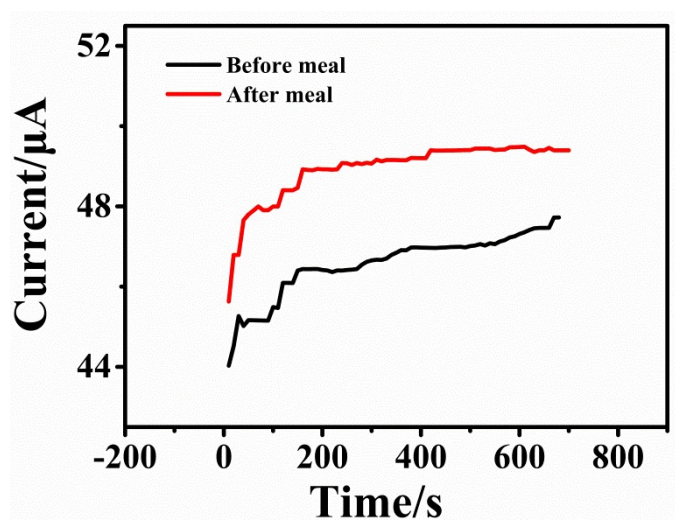


Figure S11. Comparison of sweat detection before and after meal.

Table S1. Comparison of different nanocomposite based stretchable electrochemical sensors for detection of Glucose

Electrodes	Sensitivity ($\mu\text{A}\cdot\text{mM}^{-1}\cdot\text{cm}^{-2}$)	Limit of Detection (μM)	Linear range (mM)	Ref.
CoWO ₄ /CNT on CNT/Au nanosheet patch	10.89	1.3	0.05-0.3	1
Au/PB/GOx/Ch fiber	11.7	6	0-0.5	2
GOx/Ch/Nafion on Pt-graphite patch	105	10	0-0.9	3
Cu on CNT fiber	46	50	0.05-5	4
rGO/PU-Au nanohybrid wrinkled fiber	140	~	0.001-1.0	5
Nanoporous gold (NPG) electrode	57.56	~	0.1-1.0	6
Processed wrinkled gold electrodes	750–810	~	1-10	7
GOx/PB/graphene/ gold mesh	1	10	0.01-0.7	8
GOx/chitosan/PB/ CNT/gold	2.35	~	~	9
GOx/chitosan/PB	23	3	0-0.1	10
NCAP film electrode	205.1	4.25	0.02-0.79	This work

References

1. S. Y. Oh, S. Y. Hong, Y. R. Jeong, J. Yun, H. Park, S. W. Jin, G. Lee, J. H. Oh, H. Lee, S.-S. Lee and J. S. Ha, *Acs Applied Materials & Interfaces*, 2018, **10**, 13729-13740.
2. Y. Zhao, Q. Zhai, D. Dong, T. An, S. Gong, Q. Shi and W. Cheng, *Analytical Chemistry*, 2019, **91**, 6569-6576.
3. A. Abellan-Llobregat, I. Jeerapan, A. Bandodkar, L. Vidal, A. Canals, J. Wang and E. Morallon, *Biosensors & Bioelectronics*, 2017, **91**, 885-891.
4. D. Jiang, Z. Liu, K. Wu, L. Mou, R. Ovalle-Robles, K. Inoue, Y. Zhang, N. Yuan, J. Ding, J. Qiu, Y. Huang and Z. Liu, *Polymers*, 2018, **10**.
5. T. Phan Tan, T. Tran Quang, D. Thi My Linh, C. W. Bae and N.-E. Lee, *Acs Applied Materials & Interfaces*, 2019, **11**, 10707-10717.
6. C. W. Bae, T. Phan Tan, B. Y. Kim, W. I. Lee, H. B. Lee, A. Hanif, E. H. Lee and N.-E. Lee, *Acs Applied Materials & Interfaces*, 2019, **11**, 14567-14575.
7. Y. Chan, M. Skreta, H. McPhee, S. Saha, R. Deus and L. Soleymani, *Analyst*, 2019, **144**, 1850-1850.
8. H. Lee, T. K. Choi, Y. B. Lee, H. R. Cho, R. Ghaffari, L. Wang, H. J. Choi, T. D. Chung, N. S.

- Lu, T. Hyeon, S. H. Choi and D. H. Kim, *Nature Nanotechnology*, 2016, **11**, 566-572.
9. W. Gao, S. Emaminejad, H. Y. Y. Nyein, S. Challa, K. Chen, A. Peck, H. M. Fahad, H. Ota, H. Shiraki, D. Kiriya, D.-H. Lien, G. A. Brooks, R. W. Davis and A. Javey, *Nature*, 2016, **529**, 509-514.
10. A. J. Bandothkar, W. Jia, C. Yardimci, X. Wang, J. Ramirez and J. Wang, *Analytical Chemistry*, 2015, **87**, 394-398.